Acta Cryst B
STRUCTURAL SCIENCE
CRYSTAL ENGINEERING
MATERIALS

ISSN 2052-5206

Crystallization induced by fungi and bacteria

Olga Frank-Kamenetskaya[a]* and Dmitry Vlasov[b,c]

[a]Department of Crystallography, St Petersburg State University, Universitetskaya emb. 7/9, St Petersburg, 199034, Russian Federation, [b]Department of Botany, St Petersburg State University, Universitetskaya emb. 7/9, St Petersburg, 199034, Russian Federation, and [c]Department of Mycology, Komarov Botanical Institute of the Russian Academy of Science, Professor Popova Street 2, St Petersburg, 197022, Russian Federation. *Correspondence e-mail: o.frank-kamenetskaia@spbu.ru

Received 31 May 2024
Accepted 13 November 2024

Edited by A. Katrusiak, Adam Mickiewicz University, Poland

This article is part of a collection of articles from the IUCr 2023 Congress in Melbourne, Australia, and commemorates the 75th anniversary of the IUCr.

Keywords: microbial biomineralization; carbonate and oxalate crystallization; fungi; bacteria; biotechnologies.

Crystallization induced by lithobiont microbial communities (fungi, bacteria, lichens) has received great attention in science and beyond. The studies discussed here focus on the mechanisms and factors of microbial biomineralization. The multilevel modelling approach, which made it possible to solve this interdisciplinary problem, is highlighted. The effect of chemical composition of biofilms, including acidity of the medium and cation oxidation degree, on oxalate formation is discussed. The variants of interaction between biofilm components and growing oxalate crystals are addressed. Particular attention is paid to the effect of metabolism of fungi, bacteria and their associations on carbonate and oxalate crystallization under various trophic conditions and the transitions between them. The possibility of applying the identified patterns to reveal the role of fungi and bacteria in the oxalate–carbonate pathway and in biotechnologies is considered.

1. Introduction

In recent years, the international scientific community has shown significant interest in the mechanisms of biomineralization with the participation of lithobiont microbial communities (Gadd, 2007, 2021; Frank-Kamenetskaya & Vlasov, 2023; Lai *et al.*, 2023; Vlasov *et al.*, 2023*a*): microscopic fungi (micromycetes), lichens (which also belong to fungi, as they contain a fungal component), algae and bacteria (Fig. 1).

A creative collaboration between crystallographers and biologists at St Petersburg State University allowed us to make a significant breakthrough in research into the mechanisms and factors of microbial biomineralization. The present paper is based on these findings and focuses on oxalate and carbonate crystallization induced by fungi and bacteria.

The interaction of microbial metabolism products with the environment, primarily with rock substrates, leads to biofilm mineralization (microbially induced crystallization), the patterns of which have not been studied much. The interest of the international scientific community in this issue stems not only from fundamental origins, but also from the prospect of using microbial crystallization in numerous nature-similar environmentally friendly technologies: enrichment of poor ores (Mehta *et al.*, 2010), detoxification of industrial waste (Ayilara & Babalola, 2023), oil refining (Ahmad *et al.*, 2023), bioremediation of soils and water bodies (Kour *et al.*, 2022; Gupta & Gandhi, 2023), creation of new building materials (Armstrong, 2023) or conservation and restoration of cultural heritage (Ranalli & Zanardini, 2021; Frank-Kamenetskaya & Vlasov, 2023). The interaction of fungi, lichens and bacteria with underlying rocks and associated minerals most often leads to the formation of metal oxalates $Me^{2+}[C_2O_4]\cdot nH_2O$

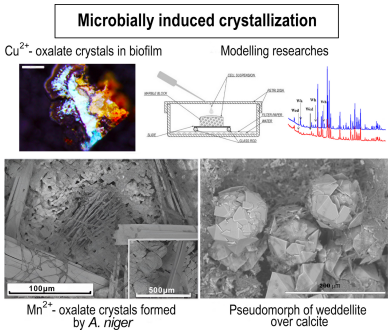

Table 1
Oxalates $Me^{2+}[C_2O_4]\ nH_2O$ in lichens (Vlasov *et al.*, 2020).

	Formula			
Mineral	Me^{2+}	n	Space-group symmetry	Underlying rocks and minerals
Whewellite	Ca^{2+}	1	$P2_1/c$	(Ca, Mg) carbonate rocks, Ca-containing minerals of silicate rocks, apatite–nepheline ore
Weddellite	Ca^{2+}	$2.5 - x$ ($x \leq 0.5$)	$I4/m$	
Moolooite	Cu^{2+}	0–1	$Pnnm$	Cu and Fe sulfides and their weathering products
Glushinskite	Mg^{2+}	2	$Fddd$	Serpentinite
Lindbergite	Mn^{2+}	2	$C2/c$	Manganese ore with manganese oxides
Andreybulachite†	Ni^{2+}	2	$C2/c$	Ni, Cu-rich sulfide ore
Katsarosite†	Zn^{2+}	2	$C2/c$	Sphalerite, jarosite, hydrozincite
No official name	Pb^{2+}	0	$P\bar{1}$	Polluted soil near a (Zn,Pb)S smelter

† New minerals discovered in the last four years have been added to the table.

(Me^{2+} = Ca, Cu, Mg, Mn, Zn, Ni) [Table 1, Figs. 2(*a*)–2(*d*)] and calcite $CaCO_3$ [Figs. 2(*e*) and 2(*f*)].

It is well known that many fungi and lichens (less often bacteria) excrete oxalic acid (Sazanova *et al.*, 2020, 2023; Vlasov *et al.*, 2020) and therefore the question of the source of oxalate ions in the crystallization medium has a definite answer. The appearance of carbonate ions in the crystallization medium is usually associated with the decomposition of organic molecules that are part of the extracellular polymer substance (EPS) excreted by bacteria (less often by fungi). Metal ions involved in the formation of oxalates and carbonates enter the crystallization medium from the environment. Most often this occurs as a result of the dissolution of

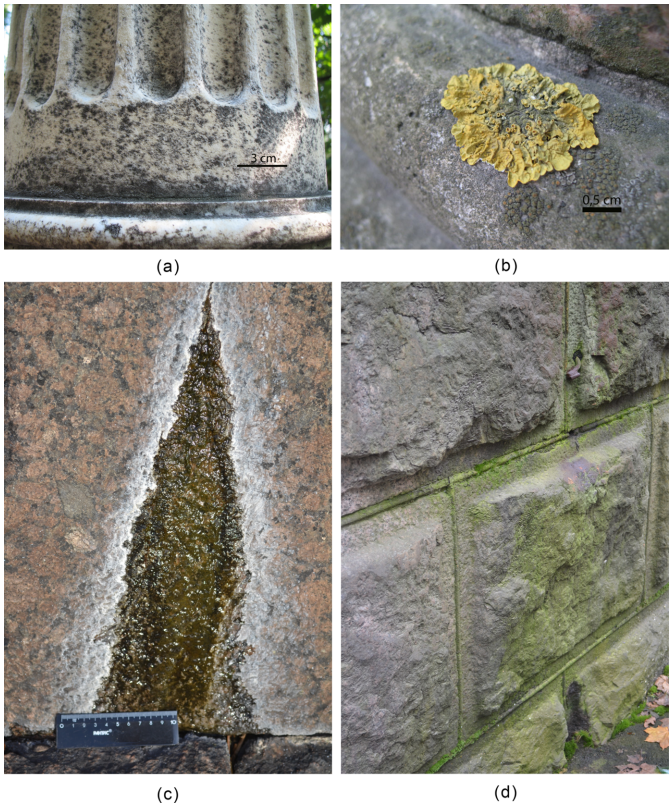

Figure 1
Biofilms on different rock substrates with a predominance of (*a*) microscopic fungi, (*b*) lichens, (*c*) cyanobacteria and (*d*) algae.

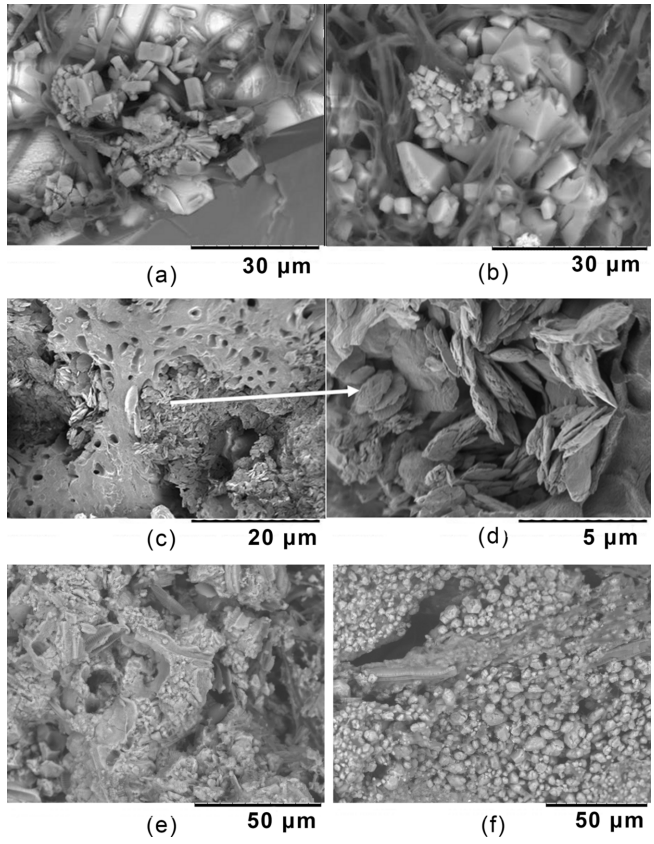

Figure 2
Crystals of oxalates and carbonates in biofilms on different rock substrates. (*a*, *b*) Fine-grain aggregates of monohydrate whewellite and dipyramidal prismatic crystals of dihydrate weddellite in the lichen *Lecanora polytropa* on apatite ore (Kola Peninsula, Russia). Reproduced with permission from Frank-Kamenetskaya *et al.* (2019*a*) under a Creative Commons Attribution 4.0 International License, https://creativecommons.org/licenses/by/4.0/. (*c*, *d*) Aggregates of copper oxalate split moolooite crystals in the lichen *Lecidea inops* on oxidized chalcopyrite ore (Voronov Bor, Karelia, Russia). The rounded ribs point to their cyclic growth and dissolution. Reproduced with permission from Frank-Kamenetskaya *et al.* (2021) under a Creative Commons Attribution 4.0 International License, https://creativecommons.org/licenses/by/4.0/. (*e*, *f*) Calcite deposits on cyanobacteria sheaths and a biofilm surface (rock art monument, Tomskaya Pisanitsa, Western Siberia, Russia). Reproduced with permission from Vlasov *et al.* (2023*b*), copyright (2023) Springer Nature.

underlying rocks under the effect of aggressive products of microbial metabolism.

2. Methodological approach

In order to clarify the mechanisms and factors of oxalate and carbonate microbial biomineralization, syntheses with the participation of fungi, bacteria and their associations on the surface of various rocks and minerals in liquid Czapek–Dox nutrient medium ($NaNO_3$ 2.0 g l^{-1}, KH_2PO_4 1.0 g l^{-1}, $MgSO_4{\cdot}7H_2O$ 0.5 g l^{-1}, KCl 0.5 g l^{-1} and $FeSO_4$ $7H_2O$ 0.01 g l^{-1}) and under oligotrophic conditions of a moist chamber were carried out. Most of the model experiments were carried out with two strains of fungi [*Aspergillus niger* (KF768341) and *Penicillium chrysogenum* (OP758843)] and the bacterium *Bacillus subtilis* (deposited under number RCAMO4920 in the RCAM collection) as well as their associations: *B. subtilis–A. niger* and *B. subtilis–P. chrysogenum.*

Under oligotrophic conditions of a moist chamber the biomineralization process was close to natural and very slow. In a liquid nutrient medium, crystallization induced by microorganisms occurred much faster than in nature, but this way we could reproduce biomineralization over a wider time interval without extending the duration of the experiment. Syntheses from aqueous solutions of known composition (with organic and inorganic components of fungi-containing biofilms) were also carried out. Preliminarily, under these experimental conditions the strains of microorganisms were selected for examining their metabolism by gas chromatography mass spectrometry (GC-MS).

The study of crystallization products was carried out using a wide range of methods, including optical microscopy, scanning electron microscopy (SEM), X-ray diffraction, Raman spectroscopy, IR spectroscopy and energy-dispersive X-ray (EDX) spectroscopy, as well as modern biological methods and approaches including genomic analysis.

3. Factors and mechanisms controlling oxalate biomineralization by fungi and lichens

3.1. The effect of chemical composition of the biofilm

The chemical composition of natural biofilms is formed under the influence of both the environment and the microorganisms (Fig. 3). The results of the synthesis of calcium oxalates by precipitation from solution at room temperature in a weakly acidic medium (as is typical for the stationary phase of micromycete growth) have shown that the chemistry of the medium, including the presence of numerous organic and inorganic impurity components which are common for biofilms on stone in an urban environment, strongly affect oxalate formation (Kuz'mina *et al.*, 2019; Rusakov *et al.*, 2021).

The decisive role in the stabilization of calcium oxalate dihydrate weddellite in the crystallization range of calcium oxalate monohydrate whewellite is played by the ratio between Ca^{2+} and $[C_2O_4]^{2-}$ ions which must be greater than one (Fig. 4). The organic acids (citric, malic, succinic and

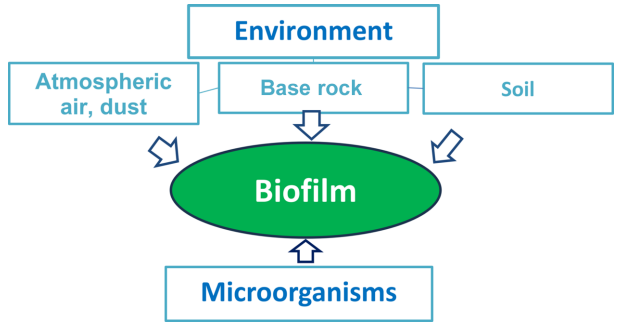

Figure 3
The ways in which elements can enter the biofilm crystallization medium.

fumaric) excreted by microscopic fungi, as well as a number of ions (K^+, Mg^{2+}, Fe^{3+}, Sr^{2+}, SO_4^{2-}, PO_4^{3-} and CO_3^{2-}) or their combinations, coming from the environment, significantly affect the weddellite/whewellite ratio (Fig. 5). However, the strongest unique effect leading to intensive weddellite crystallization is caused by the presence of citric acid in the medium and this phenomenon cannot be solely explained by the pH effect. Along with this factor, minor changes in the composition of the impurity components can lead to significant changes in the weddellite/whewellite ratio. The effect of the combination of impurities on this ratio does not obey the rule of additivity.

Lithobiont microorganisms (lichens *etc.*) not only extract elements from the underlying rocks, but also accumulate them, which contributes to the mineralization of biofilms (Sazanova *et al.*, 2021; Vereshchagin *et al.*, 2023). For example, when studying changes in the elemental composition at the boundary between basaltic rocks of Tolbachik Volcano (Kamchatka, Russia) and lichen biofilms, it was discovered that biofilm microorganisms accumulate calcium, copper and lead which are always present in the underlying basaltic rocks [Volynets *et al.* (2015) and others] and are incorporated into biofilms (Fig. 6).

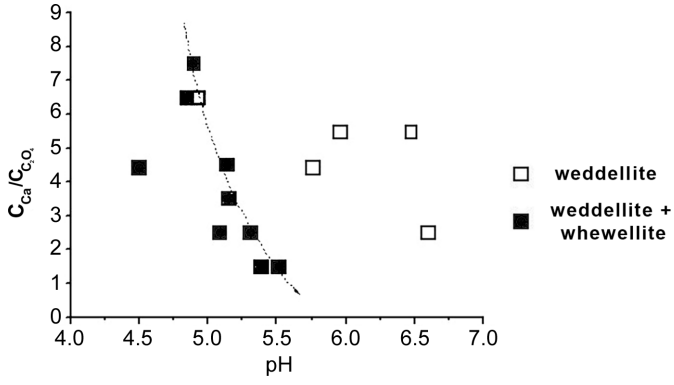

Figure 4
Crystallization of weddellite, or weddellite together with whewellite, occurring at different initial solution pH values and different ratios of the concentrations of Ca^{2+} cations and oxalate ions (C_{Ca}/C_{C2O4}) in the system with addition of the following impurity components: citrate ions (6.4 mmol l^{-1}), KCl (63.5 mmol l^{-1}) and $MgSO_4$ (3.85 mmol l^{-1}). Reproduced with permission from Kuz'mina *et al.* (2019), copyright (2019) Springer Nature.

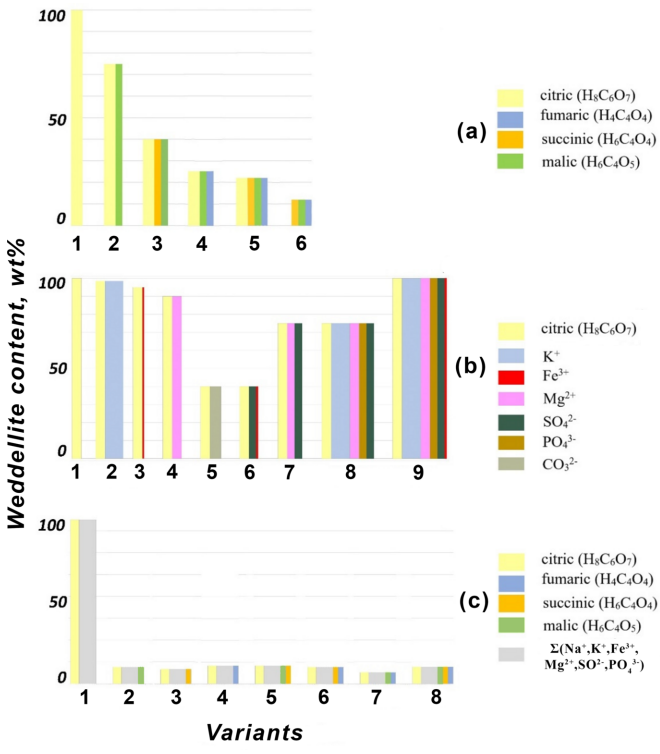

Figure 5
The content of weddellite (obtained via X-ray powder diffraction) in precipitates with different impurity components: (*a*) organic acids secreted by fungi, (*b*) citric acid and several environmental ions, and (*c*) organic acids and summed content of environmental ions. Bar width represents the relative content of the impurities in the solution. Reproduced with permission from Rusakov *et al.* (2021) under a Creative Commons Attribution 4.0 International License, https://creativecommons.org/licenses/by/4.0/.

A sharp increase in the calcium and copper content leads to oxalate formation in biofilms (Chernyshova *et al.*, 2023). Lead does not form its own oxalate phase, but the presence of lead-enriched 'nests' in areas of oxalate accumulation suggests that Pb^{2+} ions may partially substitute for Ca^{2+} and Cu^{2+} ions in calcium (whewellite, weddellite) and copper (moolooite) oxalates, and may also be adsorbed on the faces of their crystals.

Summarizing all of the above, we can conclude that the changes in the chemical composition of natural biofilms associated with environmental exposure and the activity of microorganisms significantly influence the crystallization of oxalates.

3.2. The effect of medium acidity and cation oxidation state

The formation of oxalates with metals in variable oxidation states occurred in the course of complex redox processes (Me^{2+} to Me^{3+}, Me^{4+} and *vice versa*) which depend on the oxidation state of cations leached from the underlying mineral substrate and on the pH of the crystallization medium, which is controlled not only by microbial metabolism but also by the petrographic characteristics of the underlying rock (primarily porosity) (Zelenskaya *et al.*, 2020; Frank-Kamenetskaya *et al.*, 2022). The less porous the substrate, the more the organic acids, including oxalic acid, remain on its surface. Consequently, the medium becomes more acidic and the Me^{2+}/C_2O_4 ratio decreases, which affects the phase composition of the crystallization products.

Table 2
Relative abundance of crystalline products from the reaction between Ca, Mn minerals with *A. niger versus* pH of the crystallization medium (Frank-Kamenetskaya *et al.*, 2022).

Wh denotes whewellite $Ca(C_2O_4)\cdot H_2O$, Wd weddellite $Ca(C_2O_4)\cdot 2H_2O$, L lindbergite $Mn(C_2O_4)\cdot 2H_2O$ and F falottaite $Mn(C_2O_4)\cdot 3H_2O$.

	Todorokite		Kutnohorite	
Days	Phase composition	pH	Phase composition	pH
2	Wh >> Wd	4	Wh	3.5
4	Wh >> Wd, L	4	Wh, Mn, Ca biogenic oxide	3
6	Wh >> Wd, L > F	3	Wh >> Wd, L = F, Mn,Ca biogenic oxide	2.5
8	Wh >> Wd, F	4.5	Wh, L	2
14	Wh >> Wd, F = L	6	Wh, L	2.5

As can be clearly seen from the example of oxalate crystallization under the action of *A. niger* on the surface of minerals of manganese ores (Table 2), during the experiment the pH value decreases at first and then, having reached a certain limiting value, begins to increase. This is associated with a decrease in oxalate ion content in solution due to intense crystallization and fungus culture ageing (Sturm *et al.*, 2015). The lower solubility of manganese carbonate kutnohorite (compared with the Ca,Mn-oxide todorokite) in the products of microbial metabolism slows down the processes of leaching which affects the process of phase formation, which occurs on this substrate in a more acidic medium (Table 2). In the case of calcium oxalate formation, a reduction in porosity of the underlying substrate leads to an almost complete disappearance of weddellite and an increase in whewellite content (Zelenskaya *et al.*, 2020).

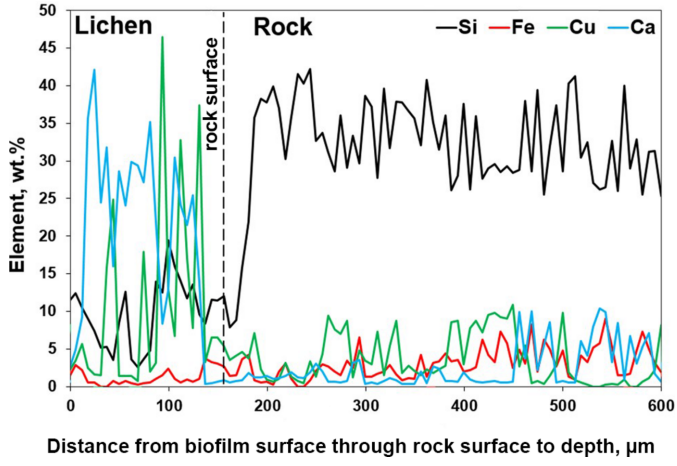

Figure 6
An example of a change in the elemental composition of a lichen-covered basaltic rock from the inside to the surface on Tolbachik Volcano (Kamchatka, Russia). Reproduced with permission from Vereshchagin *et al.* (2023), copyright (2023) Elsevier.

The patterns of the influence of the oxidation state of cations leaching from the underlying mineral substrate on oxalate formation are clearly visible during fungal crystallization on the surface of manganese and iron ores under experimental conditions (Frank-Kamenetskaya *et al.*, 2022; Zelenskaya *et al.*, 2021).

While fungi solubilize oxides containing $Me^{3+,4+}$ ions (Ca,Mn-oxide todorokite or iron sulfide pyrrhotite which is largely replaced by $Fe^{+2,+3}$ oxides), manganese and iron ions are directly released into the medium. The oxidation state of the cations then decreases to Me^{2+} and at pH $\simeq$ 3.5 the precipitation of dihydrous Me^{2+} oxalates begins with manganese oxalate lindbergite [Fig. 7(*a*), Table 2] or iron oxalate humboldtine [Figs. 8(*a*) and 8(*b*)]. Later, the trihydrous manganese oxalate falottaite appears on the surface of todorokite [Figs. 7(*b*) and 7(*c*)]. The ratio between lindbergite and falottaite varies depending on hydration and dehydration processes. The similarity of the lindbergite and falottaite crystal structures facilitates the implementation of these processes (Frank-Kamenetskaya *et al.*, 2022).

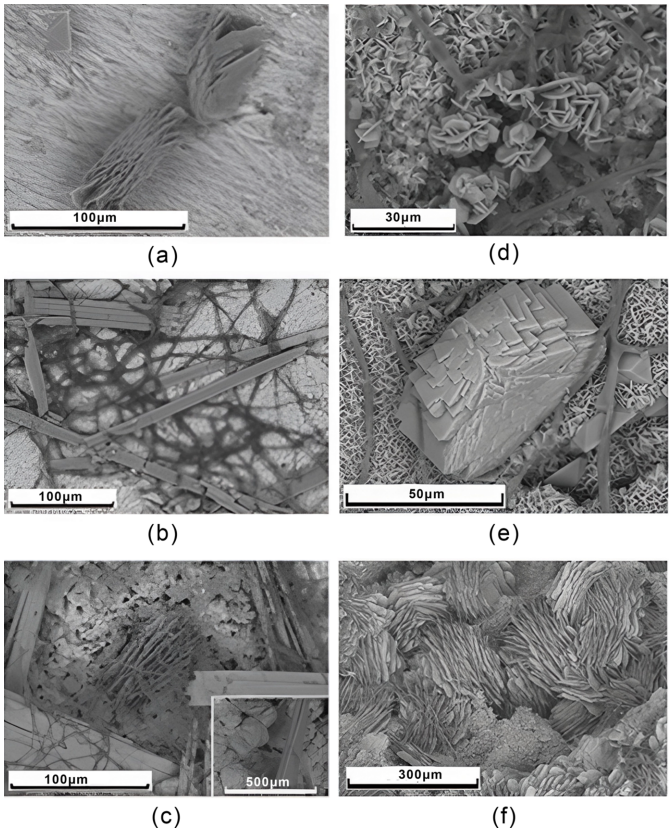

Figure 7
Manganese oxalate crystals formed by *A. niger* on (*a*)–(*c*) todorokite and (*d*)–(*f*) kutnohorite surfaces. (*a*) A large spherulite-like intergrowth of plate-like crystals of lindbergite (4th day of the experiment). (*b*) Numerous needle-like crystals of falottaite (8th day of the experiment). (*c*) Comparable amounts of lindbergite and falottaite (14th day of the experiment). (*d*) A carpet of small pseudo-hexagonal plate-like crystals of whewellite and whewellite intergrowths (2nd day of the experiment). Manganese oxide was detected by X-ray powder diffraction data. (*e*) Comparable amounts of lindbergite and falottaite (6th day of the experiment). (*f*) Intergrowths of plate-like lindbergite crystals of different generations (eighth day of the experiment). Reproduced by permission of the authors from Frank-Kamenetskaya *et al.* (2022), copyright (2022) American Mineralogical Society.

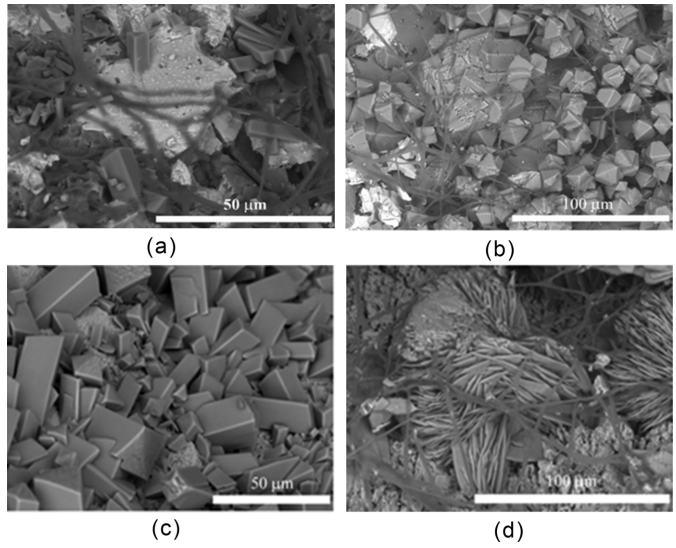

Figure 8
Humboldtine crystals formed by *A. niger* on the surface of pyrrhotite [(*a*) on the third day of the experiment and (*b*) on the eighteenth day of the experiment] and siderite [(*c*) on the fifth day of the experiment and (*d*) on the eighteenth day of the experiment]. Reproduced with permission from Zelenskaya *et al.* (2021) under a Creative Commons Attribution 4.0 International License, https://creativecommons.org/licenses/by/4.0/.

In the case of a fungus solubilizing manganese or iron carbonates (kutnohorite or siderite), the appearance of Me^{2+} ions in an acid medium at first leads to the formation of mycogenic oxide, which contains $Me^{3+,4+}$ ions (Table 2), and only after that at pH $\leq$ 3.5 does it lead to the formation of Me^{2+} oxalates: lindbergite and falottaite in the case of manganese [Figs. 7(*e*) and 7(*f*)] or humboldtine in the case of iron [Figs. 8(*c*) and 8(*d*)].

3.3. Interaction between biofilm components and forming oxalate crystals

Biofilm components (ions coming from the environment, as well as organic acids and other products of microbial metabolism) interact with formed oxalate crystals, incorporate into their crystal structure and/or adsorb on their faces.

3.3.1. Ionic substitutions

The spectrum of ionic substitutions in biofilm metal oxalates is quite wide and depends on the elemental composition of the underlying stone substrate. Very often, strontium impurities are found in biofilm calcium oxalates (whewellite and weddellite), formed on the surface of Sr-containing rocks. According to X-ray diffraction data for synthetic weddellites, Sr^{2+} ions interact with biofilm oxalates by replacing Ca^{2+} ions, which results in the formation of two series of solid solutions: isomorphic $(Ca,Sr)(C_2O_4)\cdot(2.5-x)H_2O$ (space group $I4/m$) and isodimorphic $Ca(C_2O_4)\cdot H_2O$ (space group $P2_1/c$)–$Sr(C_2O_4)\cdot H_2O$ (space group $P\bar{1}$) (Rusakov *et al.*, 2019).

Structurally related minerals of the humboldtine group (humboldtine, glushinskite and lindbergite) are solid solutions with the general formula $(Fe,Mg,Mn)C_2O_4{\cdot}2H_2O$ (Izatulina *et al.*, 2023) and form isomorphic and isodimorphic series. To date, the isodimorphic series of glushinskite $MgC_2O_4{\cdot}2H_2O$ (space group *Fddd*)–lindbergite $MnC_2O_4{\cdot}2H_2O$ (space group *C*2/*c*) has been studied in detail (Korneev *et al.*, 2022). The limiting concentration of Mn in glushinskite is roughly 20% lower than that of Mg in lindbergite, which is caused by the higher rigidity of the glushinskite structure. Besides, the crystal structure of Mn-glushinskites is characterized by violations of long-range order. The lindbergite–glushinskite transition occurs abruptly and can be classified as a first-order isodimorphic transition. The limiting concentrations of magnesium in lindbergite and manganese in glushinskite depend on the Me^{2+}/C_2O_4 ratio and the presence of citric acid in the crystallization medium.

3.3.2. Adsorption on the faces of growing crystals

Adsorbed on the faces of growing oxalate crystals, biofilm medium components significantly affect the morphology of crystals. According to the results of the syntheses of calcium oxalates from solutions containing various admixtures (see Section 3.1), the appearance and development of the faces of a tetragonal prism, characteristic of biofilm weddellite, occurs due to the inhibition of growth of this face by citric acid and other products of microbial metabolism and by some environmental ions (K^+, Sr^{2+}, CO_3^{2-} and Mg^{2+} + SO_4^{2-}) (Figs. 9 and 10) adsorbed on its surface (Rusakov *et al.*, 2016, 2021).

Table 3
Results of experiments with *B. subtilis* and *B. subtilis–A. niger* association (at 21 days): pH *versus* content of oxalic acid and EPS in a liquid nutrient medium with different glucose contents (Sazanova *et al.*, 2020).

Glucose content ($g\ l^{-1}$)	pH	Oxalic acid ($mg\ ml^{-1}$)†	EPS ($mg\ ml^{-1}$)†
B. subtilis			
1	7.8	1.0 ± 0.4	328 ± 44
5	8.2	0.6 ± 0.4	405 ± 58
10	7.4	1.1 ± 0.3	1121 ± 181
30	7.2	0.8 ± 0.1	1460 ± 204
B. subtilis–A. niger association			
1	8.0	2.0 ± 0.1	437 ± 66
10	5.0	1033 ± 89	1.1 ± 0.2
30	5.5	3275 ± 232	10 ± 2

† Standard deviations are indicated.

Another example of the influence of impurities on the morphology of minerals crystallizing under the action of fungi is associated with iron oxalate humboldtine, synthesized under *A. niger* on the minerals of iron ores – on pyrrhotite and siderite (see Section 3.2). The humboldtine crystals synthesized on pyrrhotite contained an admixture of magnesium, and those synthesized on siderite contained an admixture of manganese, which have entered from the corresponding underlying mineral substrates (Zelenskaya *et al.*, 2021). The obtained elongated humboldtine crystals containing magnesium were faceted by two prisms differently oriented with respect to the elongation [Figs. 8(*a*) and 8(*b*)]. These crystals were similar in morphology to the mineral glushinskite (magnesium oxalate dihydrate), which belongs to the humboldtine group and is structurally related to humboldtine (Izatulina *et al.*, 2023).

The spherulite-like intergrowths of humboldtine crystals obtained on siderite at later stages of the experiment contained an admixture of manganese and fully covered the siderite surface [Fig. 8(*d*)]. Such intergrowths are typical for lindbergite (Mn oxalate dihydrate) which is also structurally

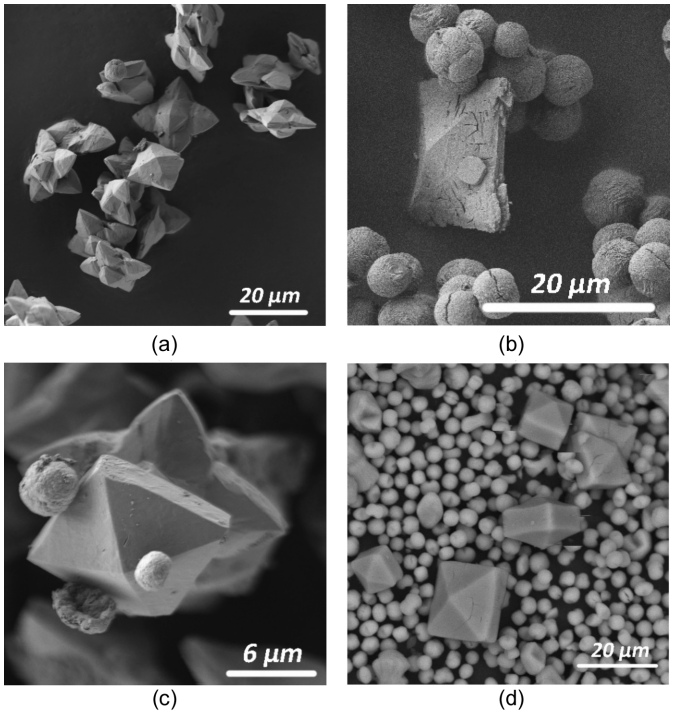

Figure 9
Tetragonal prism faces of weddellite crystals synthesized with citrate ions and some environmental ions: (*a*) with potassium cations, (*b*) with magnesium and sulfate ions, (*c*) with carbonate ions and (*d*) with strontium cations. Reproduced with permission from Rusakov *et al.* (2021) under a Creative Commons Attribution 4.0 International License, https://creativecommons.org/licenses/by/4.0/.

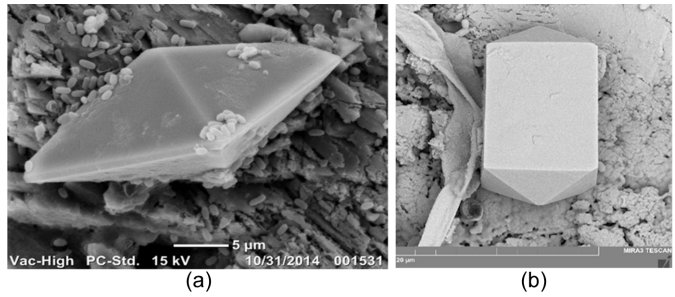

Figure 10
Weddellite crystals with varying prismatic face sizes on the surface of marble. (*a*) Prism faces are almost absent (under bacterium *B. subtilis*). (*b*) Prism faces are more prominent than dipyramidal faces (under bacterium *B. subtilis* and fungus *A. niger*). The experiment was carried out for three months in a moist chamber. Reproduced with permission from Rusakov *et al.* (2016), copyright (2016) Springer Nature.

Table 4
Results of experiments with *P. chrysogenum* and *P. chrysogenum–B. subtilis* association (at 14 days): pH *versus* content of oxalic acid and EPS in a liquid nutrient medium with different glucose contents (Sazanova *et al.*, 2023).

Glucose content ($g\ l^{-1}$)	pH	Oxalic acid ($mg\ ml^{-1}$)†	EPS ($mg\ ml^{-1}$)†
P. chrysogenum			
1	6.5	3.8 ± 0.4	Trace
10	6.0	83 ± 9	Trace
30	4.2	387 ± 13	1550 ± 62
P. chrysogenum–B. subtilis association			
1	6.5	5 ± 1	360 ± 21
10	5.7	92 ± 8	810 ± 51
30	5.5	415 ± 18	2450 ± 71

† Standard deviations are indicated.

Table 5
Results of experiments with *P. chrysogenum* and *P. chrysogenum–B. subtilis* association (at 70 days): pH *versus* content of oxalic acid and EPS in a liquid nutrient medium with different glucose contents (Sazanova *et al.*, 2023).

Glucose content ($g\ l^{-1}$)	pH	Oxalic acid ($mg\ ml^{-1}$)†	EPS ($mg\ ml^{-1}$)†
P. chrysogenum			
1	6.0	38 ± 4	388 ± 58
10	6.5	311 ± 27	1183 ± 208
30	7.0	436 ± 25	58046 ± 4008
P. chrysogenum–B. subtilis association			
1	7.0	41 ± 9	601 ± 52
10	8.0	335 ± 18	1834 ± 178
30	7.0	480 ± 32	64300 ± 8734

† Standard deviations are indicated.

related to humboldtine (Frank-Kamenetskaya *et al.*, 2022; Izatulina *et al.*, 2023).

4. Effect of microbial metabolism on crystallization under various trophic conditions

On the basis of the experiments in which the contents of organic acids (primarily oxalic) and extracellular polymeric substances (EPS) in the medium were determined, we analysed the effect of microbial metabolism on crystallization under various trophic conditions (Sazanova *et al.*, 2020, 2023).

4.1. *B. subtilis* and *B. subtilis–A. niger* association

In the case of *B. subtilis* bacterium, the conditions of the moist chamber are not favourable for EPS accumulation and secondary calcite formation. Crystals of calcium oxalate weddellite form on a marble surface [Fig. 11(*a*)]. An increase in the glucose content of the liquid medium leads to an increase in EPS release by the bacterium but barely affects the release of oxalic acid by it (Table 3). A slightly alkaline environment promotes carbonate formation [Figs. 11(*b*) and 11(*c*)]. So with the increase in nutrients in the medium, oxalate crystallization is replaced by carbonate crystallization.

Crystallization in a liquid nutrient medium under the influence of the association of the bacterium *B. subtilis* with the fungus *A. niger* occurs differently than under the influence of only the bacterium *B. subtilis* (Fig. 12). An increase in the glucose content leads to an increase in oxalic acid release by the fungus, and possibly by the bacterium itself, which reduces the pH of the medium and inhibits the release of EPS by the bacterium (Table 3). Carbonate crystallization is suppressed while oxalate crystallization is activated [Figs. 12(*b*) and 12(*c*)].

4.2. *P. chrysogenum* and *P. chrysogenum–B. subtilis* association

In the case of the fungus *P. chrysogenum*, the contents of oxalic acid and EPS increase unevenly with time as the glucose content increases (Tables 4 and 5). Oxalate crystallization is replaced by a simultaneous carbonate–oxalate crystallization when alkalization of the medium occurs (at first locally). If acidification occurs, the reverse process takes place [Figs. 13(*a*) and 14].

The association *P. chrysogenum–B. subtilis* has a synergistic effect on EPS accumulation, which contributes to the alkalization of the medium and promotes carbonate crystallization already at minimum glucose content [Tables 4 and 5, and

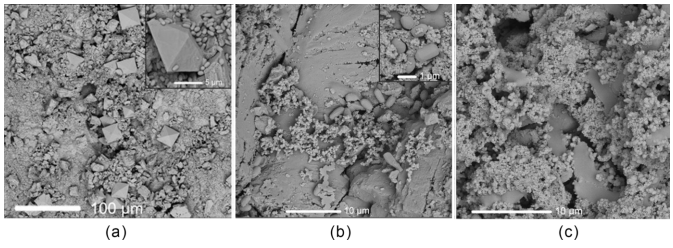

Figure 11
The crystals formed by the bacterium *B. subtilis* under different conditions on a marble surface. (*a*) Weddellite dipyramidal crystals (moist chamber, 90 days of the experiment). (*b*) Globules of secondary calcite crystals (liquid nutrient medium, glucose content 1 $g\ l^{-1}$, 30 days of the experiment). (*c*) Globules of secondary calcite crystals (liquid nutrient medium, glucose content 10 $g\ l^{-1}$, 30 days of the experiment). Reproduced with permission from Sazanova *et al.* (2020) under a Creative Commons Attribution 4.0 International License, https://creativecommons.org/licenses/by/4.0/.

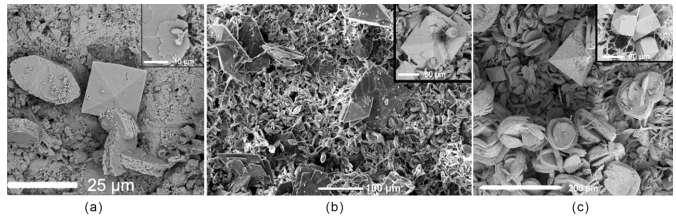

Figure 12
Crystals formed under the effect of *B. subtilis–A. niger* association on a marble surface in a liquid nutrient medium with different glucose concentrations (21 days of experiment). (*a*) Globules of secondary calcite crystals, weddellite crystals and whewellite crystal intergrowths (1 $g\ l^{-1}$). (*b*) Dipyramidal weddellite crystals in a continuous carpet of plate-like whewellite crystals (10 $g\ l^{-1}$). (*c*) Spherulitic whewellite intergrowths and weddellite crystals (30 $g\ l^{-1}$). Reproduced with permission from Sazanova *et al.* (2020) under a Creative Commons Attribution 4.0 International License, https://creativecommons.org/licenses/by/4.0/.

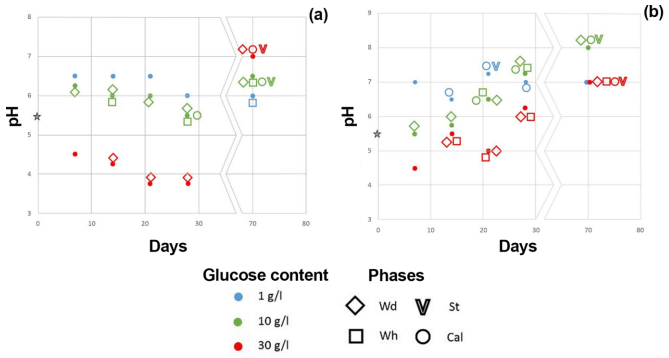

Figure 13
Phase formation at different glucose levels and pH values by the action of microorganisms, (*a*) by *P. chrysogenum* and (*b*) by *P. chrysogenum–B. subtilis* association. Here and in Figs. 14 and 15, Wd denotes weddellite, Wh whewellite, St struvite and Cal calcite. Reproduced with permission from Sazanova *et al.* (2023) under a Creative Commons Attribution 4.0 International License, https://creativecommons.org/licenses/by/4.0/.

Figs. 13(*b*) and 15(*a*)]. The presence of a pseudomorph of weddellite over calcite [Fig. 15(*d*)] is direct evidence of a possible transition from carbonate to oxalate crystallization due to a decrease in the pH of the medium effected by the metabolic products of the studied bacterial–fungal association.

The changes in composition of the metabolites excreted by the bacterium and fungus (the oxalic acid and EPS concentrations) significantly affected the pH values of the cultivation medium (Tables 3, 4 and 5, and Fig. 13). In the monoculture of *P. chrysogenum* fungus in the course of a month of cultivation (up to the moment of an abrupt increase in EPS), a significant inverse correlation between the pH values and the content of oxalic acid was observed. It was not violated even due to the presence of other organic acids in the medium at a glucose content of 30 g l^{-1}, in addition to oxalic acid. A slight alkalization at the start of the experiment (from pH 5.5 in the initial Czapek–Dox medium to pH 6.5 and 6.2 at 1 and 10 g l^{-1} of glucose content, respectively) is typical for fungi of the *Penicillium* genus and is probably associated with active ammonia excretion, which is a result of protease activation followed by the deamination of amino acids. Alkalization of the medium occurred after roughly one month of cultivation at all glucose contents, but with different intensities, and was accompanied by a slight decrease in the biomass which indicated the beginning of an autolysis processes. This allowed us to make the assumption that the significant inverse correlation between the pH value and the concentration of EPS during a month of cultivation was due to the fact that the weakly alkaline environment was more favourable for the formation of EPS by the microorganisms.

Summarizing the results of the performed experiments, we can conclude that the transition from the crystallization of oxalates to carbonates and of carbonates to oxalates (the simultaneous crystallization of oxalates and carbonates was also possible) could occur with a change in the species

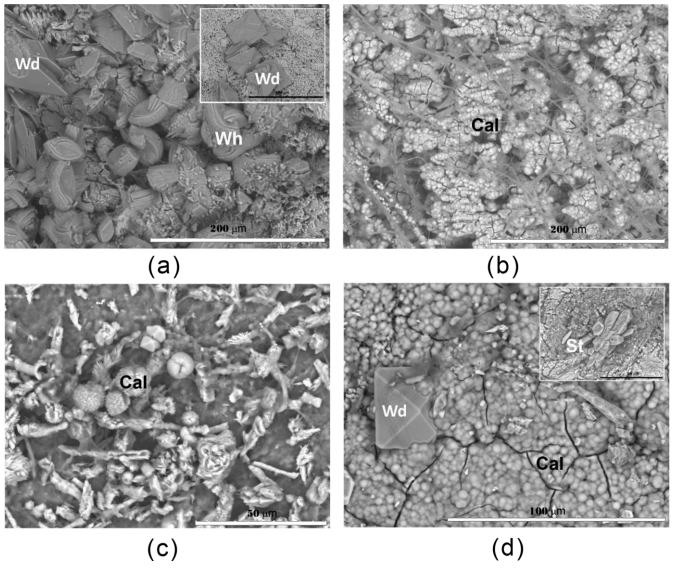

Figure 14
Crystals and their intergrowths formed on the surface of marble under the activity of *P. chrysogenum* in a liquid medium at different glucose levels. (*a*) Intergrowths of lamellar whewellite crystals and dipyramidal crystals of weddellite (glucose content of 10 g l^{-1}, 14 days of experiment). (*b*) Globules of secondary calcite on fungal hyphae (glucose content of 10 g l^{-1}, 28 days of experiment). (*c*) Large spherical intergrowths of circular calcite crystals and calcified fungal hyphae (glucose content of 10 g l^{-1}, 70 days of experiment). (*d*) A dense crust of secondary calcite globules containing weddellite crystals and intergrowths of struvite crystals (glucose content of 30 g l^{-1}, 70 days of experiment). Reproduced with permission from Sazanova *et al.* (2023) under a Creative Commons Attribution 4.0 International License, https://creativecommons.org/licenses/by/4.0/.

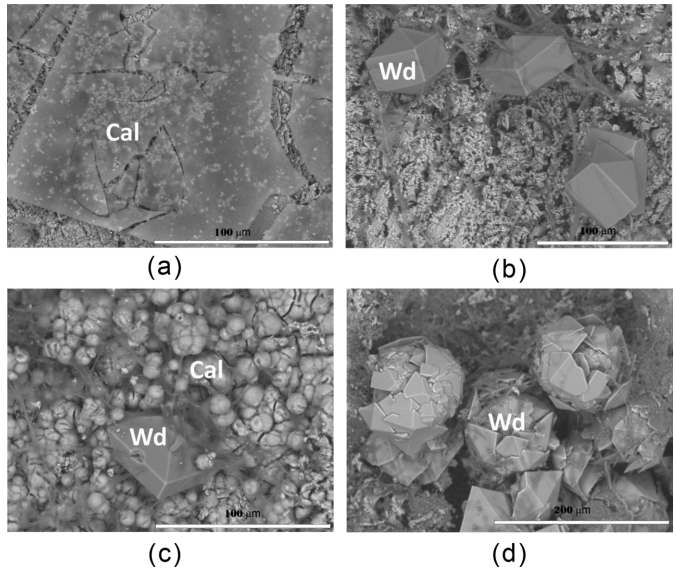

Figure 15
Crystals and intergrowths formed on a marble surface under activity of *P. chrysogenum–B. subtilis* association at different glucose levels. (*a*) A thin crust of globules of secondary calcite (glucose content of 1 g l^{-1}, 14 days of experiment). (*b*) Dipyramidal prismatic crystals of weddellite (10 g l^{-1}, 14 days of experiment). (*c*) A crust of spherical globules of secondary calcite containing dipyramidal prismatic crystals of weddellite (10 g l^{-1}, 21 days of experiment). (*d*) A pseudomorph of weddellite over calcite (10 g l^{-1}, 70 days of experiment). Reproduced with permission from Sazanova *et al.* (2023) under a Creative Commons Attribution 4.0 International License, https://creativecommons.org/licenses/by/4.0/.

composition of the lithobiont microbial community (in our case, during the transition from monocultures of the fungus *P. chrysogenum* to the bacterial–fungal association *P. chrysogenum–B. subtilis*), as well as when the nutritional value of the medium changed (in our case, when the glucose content changed). In both the *P. chrysogenum* fungus monocultures and the *P. chrysogenum–B. subtilis* association, the biomass, oxalic acid and EPS increased due to an increase in the glucose content and cultivation time. However, under the action of the bacterial–fungal association, the culture medium was alkalized and more favourable conditions for carbonate crystallization emerged. The results obtained could be used to reveal the role of fungi and bacteria in the oxalate–carbonate pathway.

5. Outlook and implications

The work presented here clearly demonstrates that an approach based on multilevel experimental simulation makes possible significant advancement in the study of the factors and mechanisms of oxalate and carbonate biomineralization with the participation of the lithobiont microbial community. There is no doubt that microbial crystallization is controlled by the chemical composition of the crystallization medium, which forms as a result of an active interaction of the metabolic products of the microorganisms with elements coming from the environment (primarily from the underlying mineral substrate). The contribution of the underlying rock to the phase composition of the products of biofilm crystallization is determined not only by its elemental composition, including the degree of oxidation of ions, but also by its petrographic characteristics. Biofilm microorganisms not only extract calcium and toxic heavy metals from the underlying rocks but also accumulate them. Biofilm chemical components that do not form their own phases are actively involved in the crystallization. They are incorporated into the structures of the formed oxalates and/or selectively adsorbed on the faces of their crystals. Variations in the nutritional components of the medium result in a change in the content of oxalic acid and EPS in the products of microbial metabolism. This significantly affects the pH of the crystallization medium and can lead to the replacement of oxalate crystallization by carbonate crystallization and *vice versa*.

The patterns identified here could be used to reveal the role of fungi and bacteria in the oxalate–carbonate pathway, as well as in the development of technologies involving microorganisms.

The effectiveness of using fungi for leaching heavy metals from ores, including low-grade industrial manganese and iron ores and in environmental bioremediation, has been shown (Frank-Kamenetskaya *et al.*, 2022; Zelenskaya *et al.*, 2021). The advantages of fungi over other microorganisms are due to the fact that fungi are able to withstand elevated concentrations of toxic elements in the environment, are easily cultivated and can quickly accumulate biomass. In addition, fungi are able to improve the properties of contaminated soils, making them more accessible to plants, which can be used in the second stage of bioremediation of contaminated objects.

In biotechnologies utilizing *B. subtilis* as well as other oxalate-producing bacteria, the time taken for crystallization and the thickness of the carbonate crust can be controlled by varying the amount of sugar in the medium (Sazanova *et al.*, 2020). At the same time, it is necessary to take precautions to prevent contamination of a marble surface by different airborne microbes. As our experience shows, regular routine care associated with chemical cleaning of the surface of marble monuments can significantly reduce the number of microorganisms (primarily microscopic fungi) on the rock surface (Frank-Kamenetskaya *et al.*, 2019*b*). After such cleaning it is possible to use 'beneficial' bacteria to restore the surface of the monument, taking into account the specific parameters of the crystallization medium.

Acknowledgements

The work was done on the basis of several St Petersburg State University resource centres: RDMI, MIM, Geomodel, RMCT and Nanotechnologies. We thank all participants of the RSF grant 19-17-00141 who contributed to this work.

References

Ahmad, A., Zamzami, M., Ahmad, V., Al-Thawadi, S., Akhtar, M. S. & Khan, M. J. (2023). *Fermentation*, **9**, 211.
Armstrong, R. (2023). *Microb. Biotechnol.* **16**, 1112–1130.
Ayilara, M. & Babalola, O. (2023). *Front. Agron.* **5**, 1183691.
Chernyshova, I., Vereshchagin, O., Zelenskaya, M., Vlasov, D., Frank-Kamenetskaya, O. & Himelbrant, D. (2023). *XIII General Meeting of the Russian Mineralogical Society and the Fedorov Session*, edited by Yu. B. Marin, pp. 17–24, https://doi.org/10.1007/978-3-031-23390-6_3. Cham: Springer Nature.
Frank-Kamenetskaya, O., Ivanyuk, G., Zelenskaya, M., Izatulina, A., Kalashnikov, A., Vlasov, D. & Polyanskaya, E. (2019*a*). *Minerals*, **9**, 656.
Frank-Kamenetskaya, O. & Vlasov, D. (2023). *XIII General Meeting of the Russian Mineralogical Society and the Fedorov Session*, edited by Yu. B. Marin, pp. 50–56, https://doi.org/10.1007/978-3-031-23390-6_7. Cham: Springer Nature.
Frank-Kamenetskaya, O., Vlasov, D., Rytikova, V., Parfenov, V., Manurtdinova, V. & Zelenskaya, M. (2019*b*). *ICAM 2019*, pp. 479–482, https://doi.org/10.1007/978-3-030-22974-0_118. Cham: Springer Nature.
Frank-Kamenetskaya, O., Zelenskaya, M., Izatulina, A., Gurzhiy, V., Rusakov, A. & Vlasov, D. (2022). *Am. Mineral.* **107**, 100–109.
Frank-Kamenetskaya, O., Zelenskaya, M., Izatulina, A., Vereshchagin, O., Vlasov, D., Himelbrant, D. & Pankin, D. (2021). *Sci. Rep.* **11**, 24239.
Gadd, G. (2007). *Mycol. Res.* **111**, 3–49.
Gadd, G. (2021). *Curr. Biol.* **31**, R1557–R1563.
Gupta, P. & Gandhi, M. (2023). *BioTech*, **12**, 36.
Izatulina, A., Kuz'mina, M., Korneev, A., Zelenskaya, M., Gurzhiy, V. & Frank-Kamenetskaya, O. (2023). *XIII General Meeting of the Russian Mineralogical Society and the Fedorov Session*, edited by Yu. B. Marin, pp. 611–618, https://doi.org/10.30695/zrmo/2023.101. Cham: Springer Nature.
Korneev, A. V., Izatulina, A. R., Kuz'mina, M. A. & Frank-Kamenetskaya, O. V. (2022). *Int. J. Mol. Sci.* **23**, 14734.

Kour, D., Khan, S., Kour, H., Kaur, T., Devi, R., Rai, P., Judy, C., McQuestion, C., Bianchi, A., Spells, S., Mohan, R., Rai, A. & Yadav, A. (2022). *J. Appl. Biol. Biotech.* **10**, 6–24.

Kuz'mina, M., Rusakov, A., Frank-Kamenetskaya, O. & Vlasov, D. (2019). *Crystallogr. Rep.* **64**, 161–167.

Lai, H., Ding, X., Cui, M., Zheng, J., Chen, Z., Pei, J. & Zhang, J. (2023). *Biogeotechnics*, **1**, 100039.

Mehta, K., Das, C. & Pandey, B. (2010). *Hydrometallurgy*, **105**, 89–95.

Ranalli, G. & Zanardini, E. (2021). *J. Appl. Microbiol.* **131**, 583–603.

Rusakov, A., Kuz'mina, M. & Frank-Kamenetskaya, O. (2021). *Molecules*, **26**, 5030.

Rusakov, A., Kuzmina, M., Izatulina, A. & Frank-Kamenetskaya, O. (2019). *Crystals*, **9**, 654.

Rusakov, A., Vlasov, A., Zelenskaya, M., Frank-Kamenetskaya, O. & Vlasov, D. (2016). *Biogenic–Abiogenic Interactions in Natural and Anthropogenic Systems*, edited by O. V. Frank-Kamenetskaya, D. Yu. Vlasov & E. G. Panova, pp. 357–377, https://link.springer.com/chapter/10.1007/978-3-319-24987-2_28. Cham: Springer Nature.

Sazanova (née Barinova), K. V., Zelenskaya, M. S., Manurtdinova, V. V., Izatulina, A. R., Rusakov, A. V., Vlasov, D. Yu. & Frank-Kamenetskaya, O. V. (2021). *Microorganisms*, **9**, 36.

Sazanova, K., Frank-Kamenetskaya, O., Vlasov, D., Zelenskaya, M., Vlasov, A., Rusakov, A. & Petrova, M. (2020). *Crystals*, **10**, 756.

Sazanova, K., Zelenskaya, M., Izatulina, A., Korneev, A., Vlasov, D. & Frank-Kamenetskaya, O. (2023). *Crystals*, **13**, 94.

Sturm, E., Frank-Kamenetskaya, O., Vlasov, D., Zelenskaya, M., Sazanova, K., Rusakov, A. & Kniep, R. (2015). *Am. Mineral.* **100**, 2559–2565.

Vereshchagin, O., Frank-Kamenetskaya, O., Vlasov, D., Zelenskaya, M., Rodina, O., Chernyshova, I., Himelbrant, D., Stepanchikova, I. & Britvin, S. (2023). *Catena*, **226**, 107048.

Vlasov, D., Frank-Kamenetskaya, O., Zelenskaya, M., Sazanova, K., Rusakov, A. & Izatulina, A. (2020). *Aspergillus niger: Pathogenicity, Cultivation and Uses*, edited by E. Baughan, pp. 1–122. New York: Nova Science Publishers.

Vlasov, D., Zelenskaya, M., Izatulina, A., Rodina, O., Vlasov, A., Sazanova, K., Vilnet, A., Abolonkova, I. & Frank-Kamenetskaya, O. (2023*a*). *Biogenic–Abiogenic Interactions in Natural and Anthropogenic Systems 2022*, edited by O. V. Frank-Kamenetskaya, D. Yu. Vlasov, E. G. Panova & T. V. Alexeeva, pp. 477–493, https://doi.org/10.1007/978-3-031-40470-2_28. Cham: Springer Nature.

Vlasov, D., Zelenskaya, M., Sazanova, K., Schigorets, S. B., Izatulina, A., Rodina, O., Stepanchikova, I., Vlasov, A., Polyanskaya, E. I., Davydov, D., Miklashevich, E., Pavlova, O. & Frank-Kamenetskaya, O. (2023*b*). *Contemp. Probl. Ecol.* **16**, 173–188.

Volynets, A. O., Edwards, B. R., Melnikov, D., Yakushev, A. & Griboedova, I. (2015). *J. Volcanology Geothermal Res.* **307**, 120–132.

Zelenskaya, M., Izatulina, A., Frank-Kamenetskaya, O. & Vlasov, D. (2021). *Crystals*, **11**, 1591.

Zelenskaya, M., Rusakov, A., Frank-Kamenetskaya, O., Vlasov, D., Izatulina, A. & Kuz'mina, M. (2020). *Processes and Phenomena on the Boundary Between Biogenic and Abiogenic Nature*, edited by O. V. Frank-Kamenetskaya, D. Yu. Vlasov, E. G. Panova and S. N. Lessovaia, pp. 581–603, https://doi.org/10.1007/978-3-030-21614-6_31. Cham: Springer Nature.